This is the accepted manuscript made available via CHORUS. The article has been published as:

Cascade of Magnetic Field Induced Spin Transitions in LaCoO_{3}

M. M. Altarawneh, G.-W. Chern, N. Harrison, C. D. Batista, A. Uchida, M. Jaime, D. G. Rickel, S. A. Crooker, C. H. Mielke, J. B. Betts, J. F. Mitchell, and M. J. R. Hoch

Phys. Rev. Lett. **109**, 037201 — Published 16 July 2012

DOI: 10.1103/PhysRevLett.109.037201

A cascade of magnetic field induced spin transitions in $LaCoO_3$

M. M. Altarawneh,[1,2] G.-W. Chern,[3] N. Harrison,[1] C. D. Batista,[4] A. Uchida,[1] M. Jaime,[1] D. G. Rickel,[1] S. A. Crooker,[1] C. H. Mielke,[1] J. B. Betts,[1] J. F. Mitchell,[5] and M. J. R. Hoch[6]

[1]*National High Magnetic Field Laboratory, Los Alamos National Laboratory, Los Alamos, NM 87545*
[2]*Department of Physics, Mu'tah University, Mu'tah, Karak, 61710, Jordan*
[3]*Theory Division, T-4 and CNLS, Los Alamos National Laboratory, Los Alamos, NM 87545*
[4]*Theory Division, Los Alamos National Laboratory, Los Alamos, NM 87545*
[5]*Material Science Division, Argonne National Laboratory, Argonne IL 60439*
[6]*National High Magnetic Field Laboratory, Florida State University, Tallahassee, FL 32310*

We present magnetization and magnetostriction studies of $LaCoO_3$ in magnetic fields approaching 100 T. In contrast with expectations from single-ion models, the data reveal *two* distinct first-order transitions and well-defined magnetization plateaux. The magnetization at the higher plateau is only about half the saturation value expected for spin-1 Co^{3+} ions. These findings strongly suggest collective behavior induced by interactions between different electronic configurations of Co^{3+} ions. We propose a model that predicts crystalline spin textures and a cascade of four magnetic phase transitions at high fields, of which the first two account for the experimental data.

PACS numbers:

Spin state crossovers induced by changes in the electronic configuration of transition metal ions can dramatically alter several materials properties [1, 2]. One example is the pressure induced spin transition of ferric ions in magnesium silicate perovskite that occurs in the Earth's lower mantle [3, 4]. Apart from being a major constituent of the Earth's mantle, perovskites exhibit a variety of behaviors which include colossal magnetoresistance [5, 6] and high temperature superconductivity [7]. For certain insulating perovskites containing Fe or Co ions, the two lowest energy multiplets of the $3d$ electrons can be separated by a small gap, Δ, owing to competition between Hund's coupling and crystal field. An external magnetic field, H, can change the electronic configuration if the lowest energy multiplet has lower spin. In this situation, structural transitions with unusually large magnetoelastic responses can be induced for $H \simeq \Delta/g\mu_B$ (μ_B is Bohr's magneton and g is the g-factor).

The gap Δ separating low- and high-spin electronic configurations of $3d$ ions in perovskites is typically of order 10-1000 meV. Controlled switching between these electronic configurations with magnetic fields therefore requires extremely large fields of order 100-10000 T (assuming $g \approx 2$). The recent development of nondestructive pulsed magnets with peak fields of 100 T and with long (ms-timescale) pulse durations now provides an opportunity to realize field-tuned spin state transitions in compounds with $\Delta \sim 12$ meV. Such studies are highly desirable, as they would provide an essential complement to pressure-induced spin cross-over phenomena that have been studied in a number of materials [8–10]. Moreover, high-field studies allow one to test whether single-ion models suffice to describe spin-crossover phenomena, or whether interactions *between* $3d$ ions are important.

To this end we study the insulating perovskite cobaltite $LaCoO_3$ (LCO), whose octahedrally-coordinated Co^{3+} ($3d^6$) ions are natural candidates to explore field-induced transitions of the electronic configuration [11, 12]. A small gap $\Delta \approx 12$ meV separates the singlet ground state (6 electrons in the t_{2g} orbitals) from the lowest energy magnetic configuration [13]. While the Co^{3+} ions are in their $S = 0$ state at low temperatures, thermal activation to a magnetic $S \neq 0$ state occurs above $\sim$30 K, giving rise to a paramagnetic response. Although considerable work has been carried out on this thermally-induced spin crossover [14–16], the spin value, S, of the first excited multiplet is still controversial. A single-ion model allows to explain the temperature dependence of the magnetic susceptibility and the measured g-factor ($g = 3.4$) with an $S = 1$ triplet [15]. Based on these preliminary results, we will assume $S = 1$ in the rest of this work. However, field-dependent magnetization studies have recently suggested that interactions between Co ions may play a crucial role: a field-induced gap-closing study shows a jump in the magnetization per Co^{3+} ion, M, to a plateau value of $\simeq 0.5\mu_B$ just above 60 T [17]. This value is much lower than the $2\mu_B$ ($4\mu_B$) expected from saturated $S = 1$ ($S = 2$) Co^{3+} ions within a single-ion model.

Very recently Platonov *et al.* [18] have reported several magnetic field-induced phase transitions in LCO single crystals at 4.2K. They apply very high fields ($\approx$ 500 T) produced by rapid ($\approx$ 15 μs) explosive compression of magnetic flux. The results show that M starts to rise significantly for $H >$ 50T, where $M \simeq 0.4\mu_B$, reaching a plateau value of $M \simeq 1.4\mu_B$ at 140 T, and a maximum value of $3.5\mu_B$ at 500 T. It is suggested that the observed plateaus and other features may be linked to antiferromagnetic interactions.[18] Smoothing of the first order transition near 60 T [17] is attributed to the rapid variation of H. No firm conclusions on the S value are presented, although it is suggested that the $S = 2$ state may be important at the highest fields reached.

Here we measure the magnetization of LCO in longer-duration non-destructive pulsed fields approaching 100 T [19]. We observe multiple magnetization steps and plateaus, which indicate the relevance of inter-ion coupling. Moreover, magnetostriction studies complement the magnetization results, and reveal large lattice changes induced by a combination of two factors: a) the S=0 and S=1 electronic configurations of the Co^{3+} ions have different volume and b) the S=1 configuration is Jahn-Teller active. High field susceptibility measurements made in a single turn pulsed field experiment reveal that the second plateau persists at least up to 140 T. We propose a model that allows for collective behavior of the Co^{3+} ions and reveals a rich phase diagram in which the plateaus originate from stable crystalline textures of $S = 1$ Co^{3+} ions in a background of $S = 0$ configurations. The orbital degree of freedom of the $S = 1$ Co ions also leads to orbital ordering (OO).

The single crystals of LCO are grown in a floating zone furnace at Argonne National Laboratory (ANL), with pieces being cut and polished into either small tapered cylinders for the M measurements, or $1 \times 1 \times 3$mm bar shaped samples for the magnetostriction experiments. $M(\mu_0 H)$ curves are obtained with an extraction magnetometer [20] and pulsed fields up to 97 T at temperatures 1.6K $\lesssim T \lesssim$55 K. High precision magnetostriction measurements are made using a fiber-optic strain gauge [21, 22]. In all experiments, singe crystals are oriented with their [010] pseudo-cubic axes parallel to H.

Figure 1(a) shows $M(\mu_0 H)$ at $T = 1.7$ K revealing two transitions accompanied by increases $\Delta M \sim 0.5\,\mu_B$, and two plateaus consistent with distinct magnetic phases. The second plateau at $M \sim 0.9\,\mu_B$ appears well below the $2\mu_B$ value expected from saturated Co^{3+} ions. Both transitions exhibit hysteresis in this pulsed field experiment. The location of the transition between rising and falling fields, as indicated by the up and down arrows, points to a diffusionless, displacive transition type [23–26]. The inset in Fig. 1(a) for fields in the range 55–63 T, and with offsets for clarity, presents an expanded view of the first transition for 1.6 K $\leq T \leq$ 55 K. The hysteresis diminishes as T is raised. Once initiated, the transitions proceed rapidly, within $\sim$ 5 μs, over the entire sample (length $\sim$ 4 mm). Figure 1(b) shows the magnetostriction parallel to the field. The transition fields and $\Delta L/L$ plateaus closely match the $M(\mu_0 H)$ behavior in Fig. 1(a). The field-induced strain $\Delta L/L \sim 10^{-3}$ exceeds that found in related perovskites [27]. For the rapidly rising fields, some rounding of the transitions is attributed to sample heating associated with latent heat release, which occurs despite immersion in superfluid ^{4}He. The observed sample expansion, $(\partial V/\partial H)_{T,P} > 0$, is consistent with the Maxwell relations because $(\partial M/\partial P)_{T,H} < 0$ for $T < 100$ K [22]. The inset in Fig. 1(b) shows $\chi = dM/dH$ at 4 K measured in a pulsed single turn magnet.

Figure 2 shows a phase diagram for LCO based on the

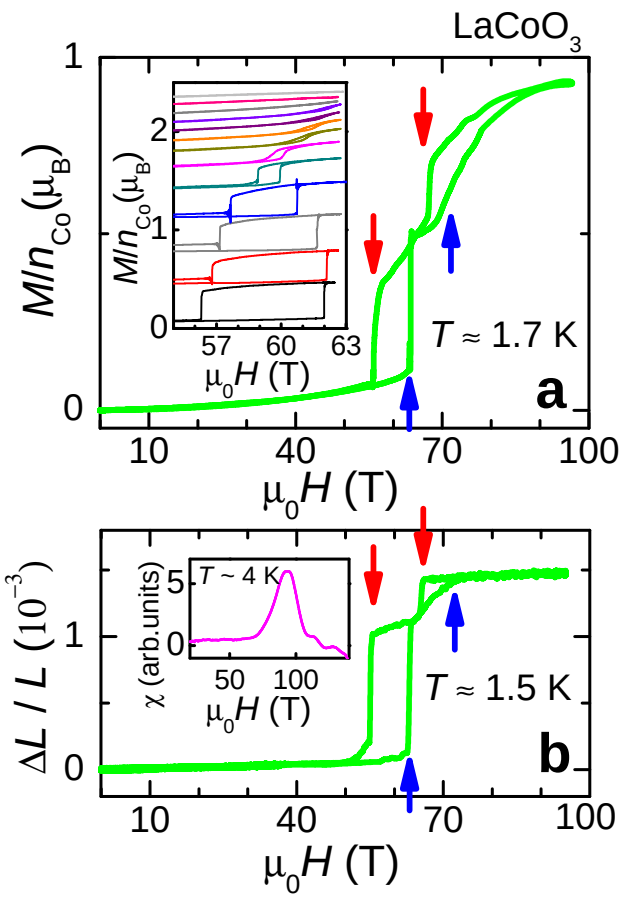

FIG. 1: (Color online) (a) Magnetization of $LaCoO_3$ in units μ_B/Co as a function of $\mu_0 H$ at $T = 1.7$ K. The up and down arrows indicate transitions for increasing and decreasing fields respectively. Two plateau regions can be seen. The inset shows an expanded view of the first transition between 55 and 63 T for T = 1.6 (bottom), 4.0, 10.0, 20.0, 25.0, 27.0, 28.0, 28.5, 29.0, 30.0, 40 and 55 (top) K. (b) Magnetostriction of LCO, measured using a high sensitivity optical strain gauge, as a function of $\mu_0 H$. The inset shows $\chi = dM/dH$ measured in a pulsed single turn coil (140 T in $\sim$ 2 μs). The two transitions are merged into a single peak in the very rapidly changing field. No further transitions are found below 140 T.

inset of Fig. 1. Besides the non-magnetic (NM) phase at low fields, there are two ordered phases denoted spin state crystalline 1 (SSC1) and 2 (SSC2). The inset depicts low-lying single-ion states for Co^{3+} in LCO [15, 17].

The observed field induced phase transitions must involve interactions between Co^3+. We note that the magnetic ions are both larger in volume as well as Jahn-Teller active [15, 17]. Indeed, the $S = +1$ Co^{3+} ion with a $t_{2g}^5 e_g^1$ electron configuration has an orbital degree of freedom because there is one electron shared between two e_g orbitals. We assume that the energy gap Δ is large in comparison to the exchange interactions between different magnetic configurations of Co^{3+} ions. We also assume that the gap to the $S = 2$ configuration is much

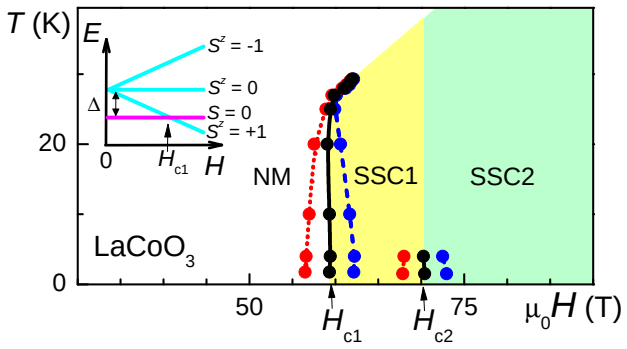

FIG. 2: (Color online) Phase diagram for LCO based on the results shown in Fig. 1(a). Blue (dashed) and red (dotted) lines denote rising and falling fields respectively, while black symbols connected by the solid curve represent the phase boundary obtained as an average of the rising and falling field values at a given T. SSC1 and SSC2 denote spin state crystalline one and two respectively. The inset shows low lying energy states as a function of applied field for Co^{3+} in LCO based on a single ion description [17].

larger than 2Δ and consequently this configuration can be eliminated from the low-energy sector for fields up to 100 T. This assumption is supported by the consistency of the model predictions with experiment. Applying a field H lowers the energy of the doubly degenerate $S^z = +1$ states (the e_g orbitals being $d_{3z^2-r^2}$ and $d_{x^2-y^2}$) such that their energy becomes comparable to the $S = 0$ state. A low-energy effective model is obtained by projecting the original Hamiltonian into the subspace of these three lowest-energy states.

The orbital state of the $S^z = +1$ ion is parameterized by an angle θ: $|\theta\rangle = \cos(\theta/2)|3z^2-r^2\rangle + \sin(\theta/2)|x^2-y^2\rangle$, corresponding to a biaxial deformation of the local O_6 octahedra. The doublet orbital degeneracy manifested as a continuous symmetry for the angle θ is retained by linear Jahn-Teller (JT) interaction. The continuous degeneracy is lifted In real compounds by the lattice anharmonicity and higher-order interactions [28]. In fact, only local elongations of the O_6 octahedra are observed in almost all JT ions with e_g electrons [29]. Depending on the local elongation axis, the allowed orbitals are $d_{3x^2-r^2}$, $d_{3y^2-r^2}$ and $d_{3z^2-r^2}$, corresponding to $\theta = 0$ and $\pm 2\pi/3$. The large nonlinear JT distortion also lifts the degeneracy of the t_{2g} levels and quenches the orbital degrees of freedom of the hole left in the t_{2g} manifold of the $S^z = 1$ state.

A single $S = 1$ ion embedded in the host matrix acquires additional energy via JT coupling with the local octahedron and exchange interaction with its nonmagnetic neighbors, amounting to a slight modification ($\tilde{\Delta}$) of the energy gap:

$$\mathcal{H}_1 = \sum_i \left(\tilde{\Delta} - g\mu_B H\right) n_i. \qquad (1)$$

Here $n_i = S_i^z = +1$ such that $n_i = 1$ for a magnetic configuration on the ion i, $\tilde{\Delta}$ is the renormalized spin state gap and $g\mu_B H$ is the Zeeman interaction. The single-ion physics described by Eq. (1) implies a single field-induced crossover when $g\mu_B H > \tilde{\Delta}$. To account for the observed multiple transitions, we need to include the interactions between the $S^z = +1$ sites:

$$\mathcal{H}_2 = \frac{1}{2}\sum_{i,j}\Big[V_{ij} + V'_{ij}(s_i, s_j)\Big] n_i n_j. \qquad (2)$$

The leading order coupling (V_{ij}) is isotropic and repulsive because it results from the increased volume of the $S^z = 1$ ions relative to the nonmagnetic ones. The second interaction terms are orbital-dependent and determine the relative orbital orientations of the magnetic ions. [21] The three-state Potts variable s_i a indicates the orbital states ($d_{3l^2-r^2}$ with $l = x$, y, or z) of the $S^z = 1$ ion. The origin of the isotropic interaction V_{ij} can be understood by using the so called "sphere-in-the-hole" model [28]. The larger ionic size of a $S = 1$ ion in the host matrix of $S = 0$ ions acts as an elastic impurity and creates a strain field which decays as $\sim 1/r^3$ at large distances. A second impurity interacts with this strain field, giving rise to the elastic term in Equation (2).

We find that the key aspects of the data – namely multiple phase transitions, incremental steps in the magnetization, lattice expansions and metastability – can be captured by considering field-induced $S^z = +1$ spin states in which we neglect orbital orientation-dependent terms. The Hamiltonian can then be mapped onto an effective Ising model

$$\mathcal{H}_{\rm eff} = J_1 \sum_{\langle ij\rangle} \sigma_i\sigma_j + J_2 \sum_{\langle\langle ij\rangle\rangle} \sigma_i\sigma_j - h\sum_i \sigma_i, \qquad (3)$$

on a cubic lattice with nearest-neighbor (NN) and next-nearest-neighbor (NNN) antiferromagnetic interactions $J_1 = V_1/4$ and $J_2 = V_2/4$, respectively, between $\sigma_i = \pm 1$ pseudospins. $S = 0$ becomes $\sigma_i = -1$ and $S^z = 1$ becomes $\sigma_i = +1$ via the transformation $n_i = (1+\sigma_i)/2$ and the adoption of an effective magnetic field $h = \frac{1}{2}g\mu_B H - \frac{1}{2}\tilde{\Delta} - \frac{3}{2}V_1 - 3V_2$ (shown schematically in Fig. 3). We note that the orbital orientation-dependent terms neglected in Eq.(3) decide the OO that accompanies each spin ordering at low enough temperatures.

Provided the NN coupling dominates (i.e. $J_1 > 4J_2$), the $h = 0$ ground state is a two-sublattice Néel order, whose actual magnetization is half of the fully saturated value, $m = \frac{1}{2}$, corresponding to $\langle\sigma_i\rangle = 0$. We associate this ordering with the measured plateau in the region above $\sim$ 75 T shown in Figs. 2 and 1. Intermediate plateaus with $m = \frac{1}{4}$ and $m = \frac{3}{4}$ (in which $\langle\sigma_i\rangle = \mp\frac{1}{2}$) become viable for finite J_2. On transforming back to the original variables, we realize a cascade of first order transitions with critical fields – H_{c1}, H_{c2}, H_{c3} and H_{c4} in Fig. 3 – whose relative separations depend on the NN and NNN repulsions V_1 and V_2.

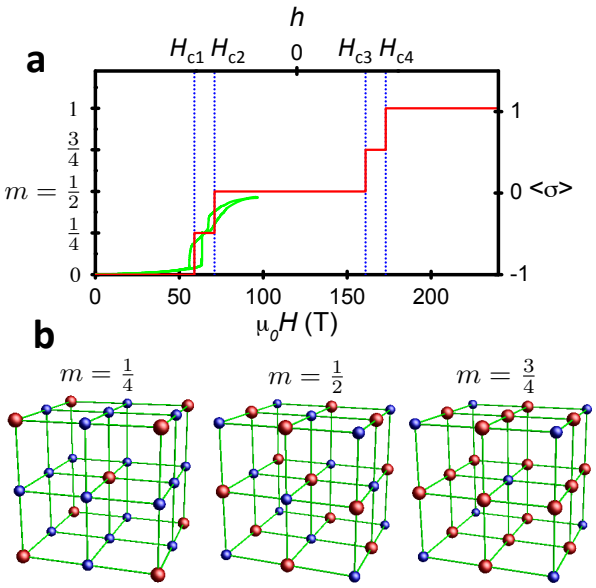

FIG. 3: (Color online) (a) The red (thin) curve is the predicted normalized magnetization curve $m(\mu_0 H)$ for LCO based on the spin model **??**eq:ising). A cascade of four transitions is shown at fields H_{c1} to H_{c4}. The scaled green (think) curve is the measured $m(\mu_0 H)$ shown in Fig. 1(a). The right hand axis gives values of the pseudospin variable $\langle\sigma\rangle$ used in the model. (b) Predicted spin state crystalline structures for each magnetization plateaux in Panel (a). The blue (larger) red balls denote Co^{3+} ions in the $S = 0$ and $S_z = +1$ states respectively. The magnetic Co ions form body-centered (BCC) and a face-centered (FCC) cubic structures in the $m = 1/4$ and $m = 1/2$ plateau regions.

Fig. 3 shows quantitative consistency between the measured magnetization steps and those of the model owing to the quenching of the orbital contribution to the g-factor (such that $g \sim 2$) by a JT distortion of the O_6 octahedra encasing the $S^z = +1$ sites. On associating the first two transitions (H_{c1} and H_{c2}) with the measured ones, we estimate $V_2 \approx 1.2$ K. The lack of further transitions in motor-generator-driven fields extending to 97 T (in Fig. 1), and in a single turn magnet system delivering fields to ≈ 140 T (shown in the inset to Fig. 1(b)), implies that $V_1 \gtrsim 25$ K. On enumerating V_1 over the six NN Co atoms in the cubic perovskite, we arrive at a lower limit $\lesssim 150$ K for the energy scale of inter-ionic exchange.

Since the $S^z = 1$ ions form a bipartite BCC structure, the dominant antiferro-orbital interaction gives rise to a staggered orbital order for the $m = 1/4$ plateau. Antiferro-orbital interactions are frustrated in the second $m = 1/2$ plateau as the $S^z = +1$ ions form a non-bipartite FCC lattice. Nonetheless, our Monte Carlo simulations found a partial OO with a layered structure.

The crystalline structures in Fig. 3(b) (e.g. BCC and FCC) anticipated for each of the phases of $LaCoO_3$ provide an explanation for the discontinuous changes in the lattice and hysteretic behavior. Each plateau in Fig. 3(a) corresponds to a different optimal sublattice arrangement of $S = 0$ and $S^z = 1$ spin states. Orbitals in the $S^z = +1$ sublattice are more voluminous and directional in nature, causing the lattice to expand in response to the pressure exerted by their increased density (i.e. V_1 and V_2). The reduced expansion at the second transition (H_{c2}) suggests the predominantly repulsive interaction is at least partially compensated by an attractive antiferro-orbital interaction, which is able to afford a more efficient arrangement of the orbitals at higher densities [21].

Finally, we reiterate that the value of S is still matter of debate [15, 30, 31]. While the generic form of the effective Ising Hamiltonian of Eq. (3) does not depend on the S value, further neighbor repulsions would be necessary to explain a $\sim 0.5\mu_B$ magnetization plateau for $S = 2$ ($\sim 0.5\mu_B$ is 1/8 of the saturated value in this case). Therefore, our original assumption of $S = 1$ leads to a simpler and more natural explanation of the measured plateaus. In addition, the orbital physics and magnetostrictive properties are very different for $S = 2$ because the e_g orbitals are not JT active.

The experimental evidence therefore suggests that collective behavior involving two spin states leads to different crystalline arrangements for increasing magnetic fields. While magnetostriction associated with field-tuned orbital order has been reported in manganites [27], the case of $LaCoO_3$ is different in that a strong spin,-orbital-lattice coupling occurs in a Mott insulator. An entirely different type of functionality results: multiple field-tuned (diffusionless) transitions giving rise to a rapidly switchable strain. Spin state crystallization is likely to be a general property of crystalline materials subject to a spin state transition under extreme conditions [3, 4, 8, 9], causing such materials to potentially become metastable in the vicinity of a phase transition and vulnerable to a sudden release of mechanical energy.

Acknowledgements. Work at the NHMFL is supported by the National Science Foundation under DMR-0654118, Florida State University, the State of Florida and the U.S. DOE BES project "Science at 100 tesla". Work at ANL is supported by the U.S. Department of Energy under Contract No. DEAC02-06CH211357.

[1] E. König, Structure and Bonding **76**, 52 (1991)
[2] A. B. Gaspar, V. Ksenofontov, M. Seredyuk, and P. Gütlich, Coord. Chem. Rev. **249**, 2661 (2005).
[3] D. Antonangeli, *et al.* Science **331**, 64 (2011).
[4] H. Hsu, P. Blaha, M. Cococcioni, and R. M. Wentzcovitch, Phys. Rev. Lett. **106**, 118501 (2011).
[5] E. Dagotto, T. Hotta, and A. Moreo, Phys. Rep. **344**, 1 (2001).
[6] M.B. Salamon and M. Jaime, Rev. Mod. Phys **73**, 583 (2001)
[7] J. R. Schrieffer and J. S. Brooks, (Eds.), *High-temperature superconductivity theory and experiment* (Springer Science, 2007).
[8] Y. Konishi, H. Tokoro, M. Nishino, and S. Miyashita, Phys. Rev. Lett. **100**, 067206 (2008).
[9] J. Miller, Physics Today **64**, 12 (2011).
[10] K. Oka, M. Azuma, W. Chen, *et al.* J. Am. Chem. Soc. **132**, 9438 (2010).
[11] P. M. Raccah and J. B. Goodenough, Phys. Rev. **155** 932 (1967).
[12] M. Johnsson and P. Lemmens, *Handbook of Magnetism and Advanced Magnetic Media.* Ed. H. Kronmller (John Wiley & Sons, New York, 2006).
[13] M. Abbate, J. C. Fuggle, A. Fujimori, *et al.* Phys. Rev. B **47**, 16124 (1993).
[14] M. A. Korotin, S. Yu. Ezhov, I. V. Solvyev, *et al.* Phys. Rev. B **54**, 5309 (1996).
[15] M. J. R. Hoch, S. Nellutla, J. van Tol, *et al.* Phys. Rev. B **79**, 214421 (2009).
[16] L. Hozoi, U. Birkenheuer, H. Stoll, and P. Fulde, New J. Phys. **11**, 023023 (2009).
[17] K. Sato, A. Matsuo, K. Kindo, Y. Kobayashi, and K. Asai, J. Phys. Soc. Jpn **78**, 093702 (2009).
[18] V. Platonov, Phys. of the Solid State **54**, 279 (2012).
[19] T. Feder, Physics Today **64**, 25 (2011).
[20] J. A. Detwiler, G. M. Schmiedeshoff, N. Harrison, *et al.* Phys. Rev. B **61**, 402 (2000).
[21] See Supplementary Information.
[22] R. Daou, F. Weickert, M. Nicklas, *et al.* Rev. Sci. Instrum. **81**, 033909 (2010).
[23] A. G. Khachaturyan, *Theory of Structural Transformations in Solids* (Dover Publications, New York 1983).
[24] R. A. Cowley, Adv. Phys. **29**, 1 (1980).
[25] M. Buerger, *Phase Transitions in Solids*, Ed. R. Smouchwski, J. E. Mayers, and W. A. Wehl, 183 (Wiley, New York, 1948).
[26] G. Hyde and O'Keefe, *Phase Transitions*, Ed. L. E. Cross, 345 (Pergamon Press, Oxford, 1973).
[27] A. Asamitsu, Y. Moritomo, Y. Tomioka, *et al.* Nature **373**, 407 (1995).
[28] D. I. Khomskii and K. I. Kugel, Phys. Rev. B **67**, 134401 (2003).
[29] K. I. Kugel and D. I. Khomskii, Usp. Fiz. Nauk **136**, 621 (1982); [Sov. Phys. Usp. **25**, 231 (1982)].
[30] A. Podlesnyak et al, Phys. Rev. Lett. **97**, 247208 (2006).
[31] T. Kyomen et al, Phys. Rev. B **71**, 024418 (2005).